Bulk superconductivity at 84 K in the strongly overdoped regime of cuprates

A. Gauzzi,[1,*] Y. Klein,[1] M. Nisula,[2] M. Karppinen,[2] P. K. Biswas,[3,†] H. Saadaoui,[3] E. Morenzoni,[3] P. Manuel,[4]
D. Khalyavin,[4] M. Marezio,[5] and T. H. Geballe[6]

[1]*IMPMC, Sorbonne Universités-UPMC, CNRS, IRD, MNHN, 4, place Jussieu, F-75005 Paris, France*
[2]*Aalto University, Department of Chemistry, FIN-00076 Espoo, Finland*
[3]*Laboratory for Muon Spin Spectroscopy, Paul Scherrer Institut, CH-5232 Villigen PSI, Switzerland*
[4]*ISIS Facility, Rutherford Appleton Laboratory-STFC, Chilton, Didcot OX11 0QX, United Kingdom*
[5]*Institut Neél, CNRS and Université Grenoble Alpes, BP 166, F-38042 Grenoble, France*
[6]*Stanford University, Department of Applied Physics & Materials Science, Stanford, California 94305, USA*

By means of magnetization, specific heat, and muon-spin relaxation measurements, we investigate newly synthesized high-pressure oxidized $Cu_{0.75}Mo_{0.25}Sr_2YCu_2O_{7.54}$, in which overdoping is achieved up to $p \sim 0.46$ hole/Cu, well beyond the T_c-p superconducting dome of cuprates, where Fermi-liquid behavior is expected. Surprisingly, we find bulk superconductivity with $T_c = 84$ K and superfluid density similar to those of optimally doped $YBa_2Cu_3O_{7-\delta}$. On the other hand, specific heat data display a large electronic contribution at low temperature, comparable to that of nonsuperconducting overdoped $La_{2-x}Sr_xCuO_4$. These results point at an unusual high-T_c phase with a large fraction of unpaired holes. Further experiments may assess the Fermi-liquid properties of the present phase, which would put into question the paradigm that the high T_c of cuprates originates from a non-Fermi-liquid ground state.

It is widely accepted that the familiar domelike dependence of the superconducting critical temperature T_c upon doped hole concentration p in the CuO_2 plane observed in most cuprates [1,2] reflects a connection between superconductivity and antiferromagnetism. T_c vanishes for $p \lesssim 0.08$ hole/Cu, as the density of mobile holes and hence the superfluid density [3] approaches zero. T_c vanishes again upon overdoping for p's larger than a critical value $p_c \approx 0.27$ hole/Cu, where the strength of the antiferromagnetic correlations also vanishes [4]. A further notion, which is generally assumed to be valid, is that the overdoped materials with $p > p_c$ behave more or less as conventional metals described by Fermi-liquid theory. In fact, this second assumption is not supported by much empirical data and it may not be correct for the first ($s = 1$) member of the homologous series of cuprates $Cu_{1-x}Mo_xSr_2(Y,Ce)_sCu_2O_{5+2s+\delta}$, originally synthesized by Ono [5] and then synthesized and characterized together with the higher members of the series up to $s = 6$ by other groups [6–12]. The high T_c's up to 87 K observed in the $s = 1$ member in the strongly overdoped region well beyond the dome put into question the paradigm that the high T_c of cuprates originates from a non-Fermi-liquid ground state [13].

In order to address this issue, in the present Rapid Communication we report a systematic investigation by means of neutron diffraction, magnetization, susceptibility, heat capacity, and muon-spin relaxation spectroscopy (μSR) on newly synthesized powders of the first ($s = 1$) member, $Cu_{1-x}Mo_xSr_2YCu_2O_{7+\delta}$, with $x = 0.25$. The structure of this phase, commonly known as (Cu,Mo)1212, is closely related to the well-known chain compound $YBa_2Cu_3O_{7-\delta}$ (Y123) with the following differences (see Ref. [9], the inset of Fig. 3, and

the Supplemental Material [14]): (1) The Ba cation is replaced by the isovalent and smaller Sr ion; (2) a fraction x of the Cu ions in the chain layers is replaced by Mo; and (3) the oxygen atoms in the chain layers are randomly distributed along the a and b directions. Consequently, the structure is tetragonal $P4/mmm$ rather than orthorhombic $Pmmm$ as in optimally doped Y123. The higher members are obtained by inserting $s - 1$ blocks of $(Y,Ce)O_2$ between the Y and CuO_2 layers into the (Cu,Mo)1212 structure.

The (Cu,Mo)1212 powder samples that are the object of this work were synthesized using the citrate sol-gel method and a modified oxidation treatment. Appropriate amounts of Y_2O_3, CuO, $SrCO_3$, and MoO_3 were dissolved in a 1M HNO_3 solution. Citric acid and ethylene glycol were added and the solution was heated in an oven at 200 °C until a gel was formed. The obtained gel was then dried, powdered, and calcined at 600 °C for 12 h. The resulting powder was pressed into a pellet and annealed at 980 °C for 2×24 h with intermediate grinding to obtain the as-synthesized product. The oxidation was carried out by mixing the as-synthesized powder with 35mol% of $KClO_3$, and the mixture was then subjected to high-pressure treatment in a cubic-anvil-type high-pressure apparatus at 4 GPa and 500 °C. The powders were first studied by means of neutron diffraction at the WISH instrument of the ISIS facility at the Rutherford Appleton Laboratory. Rietveld refinement of the neutron diffraction data yields an oxygen content $\delta = 0.54$. The only impurity phases detected in the sample are the electronically inactive KCl (4.5%) and $KClO_3$ (0.5%) arising from the oxidizing agent. The very low background noise of the WISH diffractometer [15] used for the present study enables us to rule out impurity concentrations >1%.

The superconducting transition of the powders was studied by means of dc magnetization measurements as a function of temperature in both zero-field-cooling (ZFC) and field-cooling (FC) modes at 100 Oe using a commercial superconducting quantum interference device (SQUID) Quantum Design

---

*andrea.gauzzi@upmc.fr
†Present address: ISIS Facility, Rutherford Appleton Laboratory-STFC, Chilton, Didcot OX11 0QX, United Kingdom.
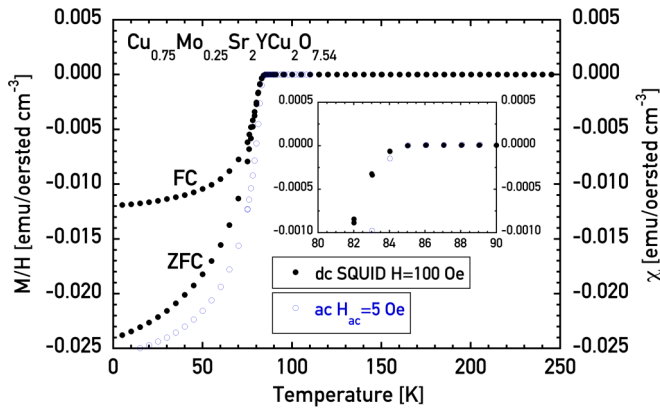
A. GAUZZI *et al.*

FIG. 1. Zero-field-cooling and field-cooling (ZFC, FC) magnetization (solid symbols) and ac susceptibility χ (open symbols) of high-pressure oxidized (Cu,Mo)1212 powders. The two curves are compared using the same scale as the small dc field of 100 Oe allows one to approximate M/H with χ. The inset shows a closeup of the transition.
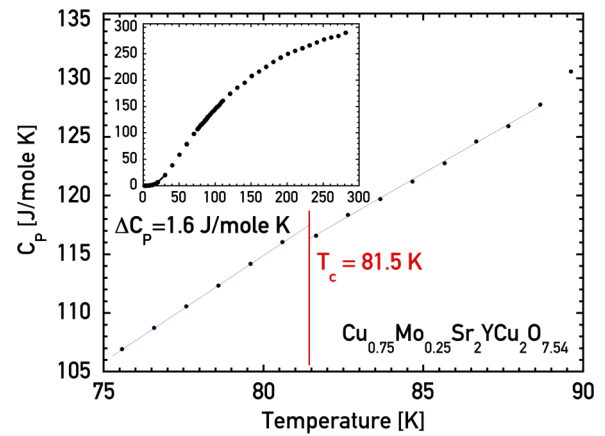

FIG. 2. Isobaric specific heat $C_p(T)$ measured on the same (Cu,Mo)1212 powder sample of Fig. 1. The main panel is a closeup of the transition showing the jump at T_c. The inset shows the behavior in the whole 2–300 K temperature range measured.

apparatus. In order to estimate more precisely the superconducting fraction, complementary measurements of ac magnetic susceptibility at a weak $H = 5$ Oe field were also carried out using a commercial physical property measurement system (PPMS) Quantum Design apparatus. A complementary study of the superconducting transition and of the electronic spectrum was carried out by means of specific heat measurements in the 2–300 K range performed using the relaxation rate method implemented in the same PPMS apparatus. Finally, the local properties of the superconducting state were probed by means of muon-spin relaxation spectroscopy. The experiments were performed on the GPS and Dolly instruments at the Swiss Muon Source SμS of the Paul Scherrer Institute. μSR is a powerful technique to determine the effective superfluid density and its temperature dependence. By applying a magnetic field perpendicular to the initial muon-spin polarization, the inhomogeneous field distribution in the vortex state of the superconductor produces a damping of the μSR precession signal expressed by the muon-spin relaxation rate $\sigma = \gamma_\mu \sqrt{\langle \Delta B^2 \rangle}$, where γ_μ is the muon gyromagnetic ratio. From the width of the magnetic field distribution in the vortex state $\sqrt{\langle \Delta B^2 \rangle}$, the magnetic penetration depth λ and its temperature dependence are determined, which is related to the effective superfluid density $\rho_s = \frac{n_s}{m^*} \propto \lambda^{-2} \propto \sigma$, where n_s is the density of superconducting electrons and m^* is their effective mass. Muon-spin rotation spectra in the vortex state were taken as a function of increasing temperature by initially field cooling the sample down to 1.6 K in different fields and analyzed assuming a Gaussian field distribution with relaxation rate σ.

In Fig. 1, we report the results of the dc magnetization and ac susceptibility measurements. Note the good agreement between the ZFC curve of the dc and ac data. Moreover, the ZFC dc magnetization curve is in fact a FC curve due to a small residual field ≈ 2 Oe trapped in the superconducting magnet. Both data sets yield a $\approx 30\%$ screening volume; the slightly smaller diamagnetic signal of the dc data is attributed to the comparatively higher field of 100 Oe used, which

leads to a larger flux penetration. As discussed in the past [16,17], the above shielding fraction is typical for single-phase superconducting cuprates that depends upon various effects, including flux pinning, among others. In the present case, considering the absence of impurities, this fraction should be then regarded as a lower limit for the Meissner fraction. We conclude that superconductivity is a bulk phenomenon associated with the oxidized $Cu_{1-x}Mo_xSr_2YCu_2O_{7+\delta}$ phase. Further evidence of bulk superconductivity is given in Fig. 2, where one notes the characteristic jump ΔC_p at T_c of the specific heat measured on the same powder sample with $T_c = 84$ K of Fig. 1 and by the μSR results to be discussed below. From Fig. 2, one obtains $\Delta C_p/T_c \approx 20$ mJ/mol K^2, a value comparable with those previously reported on other cuprate superconductors [18]. For example, $\Delta C_p/T_c \approx 11$ (50) mJ/mol K^2 in underdoped (optimally doped) Y123, with $T_c = 60(90)$ K. The slightly lower T_c value of the specific heat results is attributed to the lower accuracy within ± 1 K inherent to the relaxation method used.

The present data enable us to extend to higher T_c's the inverse dependence of T_c as a function of the c-axis parameter previously reported by Ono [5] for a series of (Cu,Mo)1212 samples with a similar, $x = 0.20$, Cu/Mo substitution level and with different oxygen doping (see Fig. 3). While this dependence is characteristic of cuprates, as it reflects the decrease of the copper-apical oxygen distance d_{ap} upon hole doping, in the present oxidized (Cu,Mo)1212 sample, this distance is strikingly short. The neutron diffraction data presented in the Supplemental Material show that superconductivity is introduced by the above high-pressure oxygen treatment while d_{ap} is reduced from 2.29 to 2.165 Å. For comparison, in Y123, d_{ap} decreases from 2.47 Å in the reduced insulating phase $YBa_2Cu_3O_6$ to 2.29 Å in optimally doped $YBa_2Cu_3O_{6.95}$ [19]. Such a record short 2.165 Å distance concomitant to a very high T_c is surprising in the following two aspects:

(1) It indicates an exceptionally large hole concentration in the CuO_2 planes, well above the maximum found in Y123 and well inside the overdoped region of cuprates. Using a self-consistent bond valence sum (BVS) analysis, where a
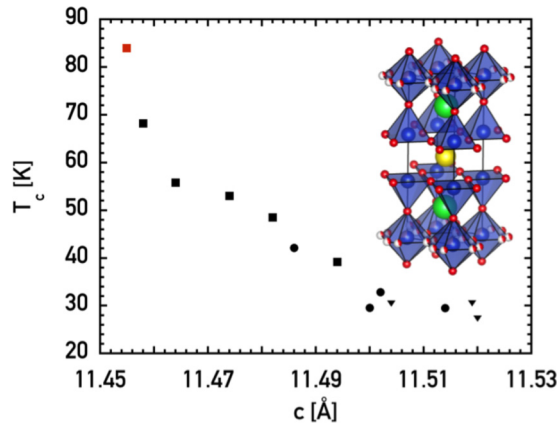
FIG. 3. Correlation between T_c and the c-axis parameter for a series of $Cu_{1-x}Mo_xSr_2YCu_2O_{7+\delta}$ samples prepared under different conditions. The red solid square corresponds to the present result obtained on a $x = 0.25$ high-pressure (HP) oxidized sample. Black symbols indicate previous results by Ono [5] on $x = 0.20$ annealed HP samples (squares), HP samples (circles), and starting samples prepared at ambient pressure (triangles). The crystal structure is shown in the inset; blue, green, yellow, and red spheres indicate Cu/Mo, Sr, Y, and oxygen atoms, respectively; white-red spheres indicate partially occupied oxygen sites in the basal plane. The structure is described in detail in Ref. [9] and in the Supplemental Material.
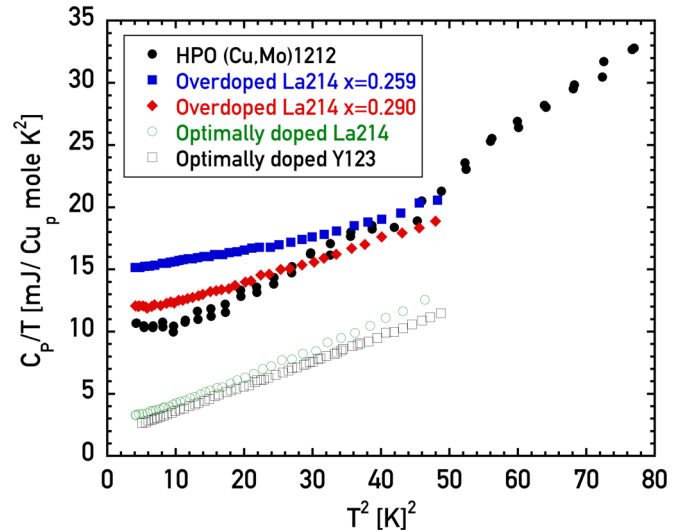

FIG. 4. Comparison of the low-temperature specific heat of the high-pressure oxidized (HPO) (Cu,Mo)1212 sample of the previous figure (black dots) with previously reported data on overdoped $La_{2-x}Sr_xCuO_4$ with $x = 0.259$ ($T_c = 6.5$ K, blue squares) and $x = 0.290$ (nonsuperconducting, red diamonds) and on optimally doped $La_{2-x}Sr_xCuO_4$ with $x = 0.178$ (green open circles) and $YBa_2Cu_3O_{7-\delta}$ with $\delta = 0.05$ (black open squares). La214 and Y123 data are taken from Refs. [24,25], respectively.

weighted value of the radius parameters, $R_0^{2+} = 1.655$ Å and $R_0^{3+} = 1.735$ Å for the Cu^{2+} and Cu^{3+} ions, respectively, has been used [9], we estimate a planar Cu valence $v_{Cu} = 2.40$. This estimate is fully consistent with the value $v_{Cu} = 2.46$ reported in previous structural [9] and x-ray absorption near edge structure (XANES) [8] studies on similar superconducting Mo-cuprate samples.

(2) The occurrence of superconductivity with T_c as high as 84 K concomitant to the above record short d_{ap} is at odds with the empirical observation that cuprate families with higher T_c's rather display longer d_{ap}'s [20], which has been supported by first principles calculations within the Hubbard model [21,22]. The present finding may therefore point at a different physics governing the strongly overdoped region of cuprates.

A picture of overdoping is supported by a straightforward analysis of the low-temperature behavior of the specific heat shown in Fig. 4. It is recalled that, in normal metals, the Sommerfeld constant γ, experimentally measured as the residual value at $T = 0$ K of the $C(T)/T$ vs T^2 curve, is proportional to the carrier density n. In a superconducting metal, γ is expected to vanish at zero temperature, and an estimate of n from the specific heat requires knowledge of the gap spectrum. In BCS d-wave superconductors such as cuprates, the existence of lines of nodes in the gap function $\Delta_\mathbf{k}$ gives rise to a parabolic increase of the specific heat at low temperature [23]. In this case, γ is related to the curvature of the parabola and its determination requires precise knowledge of the angular dependence of $\Delta_\mathbf{k}$ and of the quasiparticle spectrum [23,24].

In the analysis of the present specific heat data, we adopt a simpler approach, because the low-temperature $C(T)$ curve does not exhibit a clear parabolic dependence. The

$C(T)/T$ vs T^2 plot in Fig. 4 is flat at low temperature as if the gapless behavior was less pronounced than in the d-wave case. We then limit ourselves to compare the present data with those previously reported on optimally doped Y123 ($T_c = 92$ K) [25] and optimally doped and overdoped $La_{2-x}Sr_xCuO_4$ (La214) single crystals [24], with T_c values ranging from the maximum $T_c \approx 35$ to 0 K. Our data exhibit a very large residual electronic specific heat normalized to the number of planar Cu atoms, $\gamma \approx 10$ mJ K^{-2} Cu mol^{-1}, about four to five times larger than the values reported on the above optimally doped systems. The present value is rather comparable to the values found in overdoped La214, with vanishing T_c, or even beyond in the metallic nonsuperconducting phase, where γ probes the density of states of *normal* electrons. This conclusion is supported by similar results on optimally doped $Bi_2Sr_2CaCu_2O_8$ [26] and overdoped $Tl_2Ba_2CuO_{6+\delta}$ [27].

As to the origin of such a large γ, we rule out extrinsic effects such as a contribution of metallic impurities, as their amount is below the detection limit $\sim$1% of powder neutron diffraction. Further evidence of an electronically homogeneous phase is given by the μSR data. The data were obtained on a (Cu,Mo)1212 powder sample prepared and oxidized under the same conditions as the previously discussed sample and with the same $T_c = 84$ K. μSR is a phase volume sensitive technique and muons uniformly and locally probe the sample. So, if the sample contained different spatially separated phases, the muon signal would be the sum of different components, each component with its own precession frequency and broadening. In our sample we do not observe this behavior; the data can be fitted by a single precession signal with an amplitude corresponding to a 80% superconducting
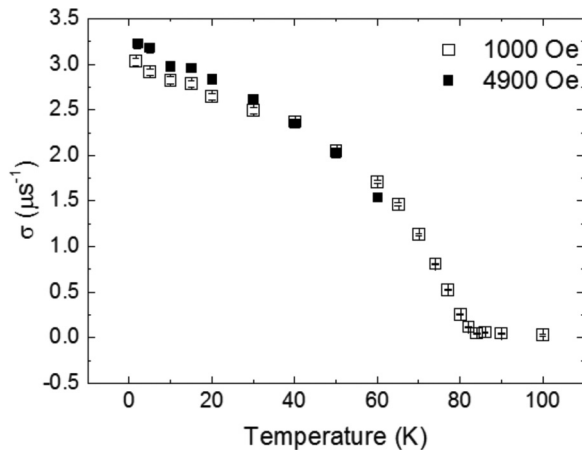
FIG. 5. Temperature dependence of the μSR rate σ at two different magnetic fields for an oxidized (Cu,Mo)1212 powder sample similar to that of Figs. 1 and 2.

fraction in the vortex state, a Gaussian relaxation rate σ, and a background contribution. Figure 5 shows the temperature dependence of σ, which is proportional to the superfluid density. Note that measurements taken at different fields display a weak temperature dependence, as expected in an extreme type-II superconductor. At low temperature, $\sigma(0) = 3.0 \pm 0.1 \ \mu s^{-1}$, very close to that measured in optimally doped Y123 [28]. At low temperatures, the linear decrease of σ with temperature is also typical of a d-wave pairing symmetry. Overall, the μSR data show that the sample is superconducting and homogeneous at least on length scales of $\sim 1 \ \mu$m corresponding to a few magnetic penetration depths. What we cannot exclude are inhomogeneities on much shorter length scales.

Having excluded the possibility of secondary phases or of other inhomogeneities on the microscopic length scale, the existence of a high-temperature superconducting phase where simple metal physics is expected is our most important finding. In characterizing the super-

conducting state, several other striking features become apparent:

(1) As in other clean cuprates, at low temperatures compared to T_c, the superfluid density decreases linearly with temperature. Generally, this is associated with the existence of nodal quasiparticles, as in the case of a clean, d-wave superconductor, which gives indirect evidence that even in this highly overdoped regime, the system is a d-wave superconductor.

(2) Reconciliation of the μSR and heat capacity data puts tight constraints on an acceptable model. At the lowest temperatures we can probe, there remains a T-linear term in the specific heat with a finite intercept showing the presence of noncondensed holes in the superconducting state. In order to avoid proximity-induced condensation, this requires that these holes should be confined in regions larger than the coherence length, $\xi \sim 10$ nm, but smaller than the penetration length, as discussed above. A scenario of a partial hole condensation in hole overdoped cuprates is supported by earlier specific heat data on overdoped La214 single crystals [24] and, more recently, by kinetic inductance measurements on well-characterized La214 single-crystal films, with $p = 0.295$, i.e., at the edge of the dome [29].

The question arises whether the failure of complete condensation of the carriers in hole overdoped cuprates may be a more general phenomenon than has been realized. In order to verify this possibility, more studies on the (Cu,Mo)1212 phase are required. For example, it would be highly desirable to vary oxygen doping and to obtain single crystals, which are needed for transport and spectrocopic investigations. In alternative, we suggest that the epitaxial growth of thin films should be investigated.

[1] H. Zhang and H. Sato, Phys. Rev. Lett. **70**, 1697 (1993).

[2] J. L. Tallon, C. Bernhard, H. Shaked, R. L. Hitterman, and J. D. Jorgensen, Phys. Rev. B **51**, 12911 (1995).

[3] V. J. Emery and S. A. Kivelson, Nature (London) **374**, 434 (1995).

[4] R. J. Birgeneau, D. R. Gabbe, H. P. Jenssen, M. A. Kastner, P. J. Picone, T. R. Thurston, G. Shirane, Y. Endoh, M. Sato, K. Yamada, Y. Hidaka, M. Oda, Y. Enomoto, M. Suzuki, and T. Murakami, Phys. Rev. B **38**, 6614 (1988).

[5] A. Ono, Jpn. J. Appl. Phys. **32**, 4517 (1993).

[6] Y. Morita, T. Nagai, Y. Matsui, H. Yamauchi, and M. Karppinen, Phys. Rev. B **70**, 174515 (2004).

[7] I. Grigoraviciute, M. Arai, H. Yamauchi, and M. Karppinen, Solid State Commun. **137**, 601 (2006).

[8] I. Grigoraviciute, M. Karppinen, T.-S. Chan, R.-S. Liu, J.-M. Chen, O. Chmaissem, and H. Yamauchi, J. Am. Chem. Soc. **132**, 838 (2010).

[9] O. Chmaissem, I. Grigoraviciute, H. Yamauchi, M. Karppinen, and M. Marezio, Phys. Rev. B **82**, 104507 (2010).

[10] M. Marezio, O. Chmaissem, C. Bougerol, M. Karppinen, H. Yamauchi, and T. H. Geballe, APL Mater. **1**, 021103 (2013).

[11] M. Marezio, O. Chmaissem, C. Bougerol, M. Karppinen, H. Yamauchi, and T. H. Geballe, J. Phys.: Conf. Ser. **507**, 012031 (2014).

[12] Non-single-phase compounds of the homologous series were also reported by Marik *et al.* [30,31] perhaps because Mo metal rather than MoO$_3$ has been used as precursor, which could explain why the samples were found to contain Mo^{5+}.

[13] Y. Ando, G. S. Boebinger, A. Passner, N. L. Wang, C. Geibel, and F. Steglich, Phys. Rev. Lett. **77**, 2065 (1996).

[14] See Supplemental Material at http://link.aps.org/supplemental/10.1103/PhysRevB.94.180509 for a detailed description of the neutron diffraction experiment and of the refined structure.

[15] L. C. Chapon, P. Manuel, P. G. Radaelli, C. Benson, L. Perrott, S. Ansell, N. J. Rhodes, D. Raspino, D. Duxbury, E. Spill, and J. Norris, Neutron News **22**, 22 (2011).

[16] K. Kitazawa, Y. Tomioka, T. Hasegawa, K. Kishio, M. Naito, T. Matsushita, I. Tanaka, and H. Kojima, Supercond. Sci. Technol. **4**, S35 (1991).

[17] C. Allgeier and J. S. Schilling, Phys. Rev. B **48**, 9747 (1993).

[18] D. R. Harshman and A. P. Mills, Phys. Rev. B **45**, 10684 (1992).

[19] R. Cava, A. Hewat, E. Hewat, B. Batlogg, M. Marezio, K. Rabe, J. Krajewski, W. Peck, and L. Rupp, Physica C **165**, 419 (1990).

[20] Y. Ohta, T. Tohyama, and S. Maekawa, Phys. Rev. B **43**, 2968 (1991).

[21] E. Pavarini, I. Dasgupta, T. Saha-Dasgupta, O. Jepsen, and O. K. Andersen, Phys. Rev. Lett. **87**, 047003 (2001).

[22] C. Weber, C. Yee, K. Haule, and G. Kotliar, Europhys. Lett. **100**, 37001 (2012).

[23] N. Momono and M. Ido, Physica C **264**, 311 (1996).

[24] Y. Wang, J. Yan, L. Shan, H.-H. Wen, Y. Tanabe, T. Adachi, and Y. Koike, Phys. Rev. B **76**, 064512 (2007).

[25] K. A. Moler, D. L. Sisson, J. S. Urbach, M. R. Beasley, A. Kapitulnik, D. J. Baar, R. Liang, and W. N. Hardy, Phys. Rev. B **55**, 3954 (1997).

[26] A. Junod, K.-Q. Wang, T. Tsukamoto, G. Triscone, B. Revaz, E. Walker, and J. Muller, Physica C **229**, 209 (1994).

[27] J. W. Loram, K. A. Mirza, J. M. Wade, J. R. Cooper, and W. Y. Liang, Physica C **235–240**, 134 (1994).

[28] Y. J. Uemura, G. M. Luke, B. J. Sternlieb, J. H. Brewer, J. F. Carolan, W. N. Hardy, R. Kadono, J. R. Kempton, R. F. Kiefl, S. R. Kreitzman, P. Mulhern, T. M. Riseman, D. L. Williams, B. X. Yang, S. Uchida, H. Takagi, J. Gopalakrishnan, A. W. Sleight, M. A. Subramanian, C. L. Chien, M. Z. Cieplak, G. Xiao, V. Y. Lee, B. W. Statt, C. E. Stronach, W. J. Kossler, and X. H. Yu, Phys. Rev. Lett. **62**, 2317 (1989).

[29] I. Božović, X. He, J. Wu, and A. T. Bollinger, Nature (London) **536**, 309 (2016).

[30] S. Marik, A. J. D. Santos Garcia, E. Morán, O. Toulemonde, and M. A. Alario-Franco, J. Phys.: Condens. Matter **25**, 165704 (2013).

[31] S. Marik, A. J. D. Santos-Garcia, C. Labrugere, E. Morán, O. Toulemonde, and M. A. Alario-Franco, Supercond. Sci. Technol. **28**, 045007 (2015).